ANALOGY-BASED MATHEMATICAL MODEL OF REINFORCED AND PRESTRESSED CONCRETE MEMBERS

By

G. TASSI

Department of Reinforced Concrete Structures, Technical University, Budapest

(Received August 3, 1977)

1. Introduction

Fundamental relationships of the classic theory of reinforced concrete ([1]) and of the theory of plasticity ([2]) helped to solve many fundamental problems of the analysis of reinforced concrete members. In the case of elements or parts of them subject to local stresses, where diaphragm effect or the effect of spatial stress state, or even the relative shift of concrete and reinforcement parts originally in the same section must not be ignored, the starting conditions are more complex. Also homogeneous, elastic discs may have a closed-form solution but in some special cases alone (e.g. [5]), and discontinuity due to cracking can only be considered under given conditions (e.g. [6]) or with partial solutions ([16]), even using the latest practical methods.

Now, a computation method for the analysis of so-called delicate domains — surroundings of e.g. application point of forces transmitted on restricted areas or surroundings of cracks — will be described.

The character of this problem excludes anything but a finite model. Earlier studies (e.g. [27], [3], [11], [17]) including those by the author ([21], [25]) applied the method of finite elements in some cases involving problems of reinforcement, cracking, non-linearity. This study, in order to gain certain advantages, extends the framework analogy to cases of reinforced or even cracked members. This refers to uses in non-linearity problems, too.

2. The framework analogy principle underlying the model

The method based on framework analogy — replacing the one-, two- and three-dimensional continuum by a discrete model ([12], [13], [15], [18]) essentially consists in constructing the investigated continuum of properly arranged bars of adequate stiffness creating an analogy between stress-strain conditions of the continuum and its model of bars. The method has its limitations, mainly as concerns the Poisson's ratio as pointed out in papers on bar structures replaced by continua ([10], [14]).

The investigated plane redundant models corresponding to isotropy exhibit a greater difference ($\nu = 1/3$), spatial models with secondary plane members a lesser one ($\nu = 1/4$) compared to Poisson's ratios usual for reinforced concrete structures. Investigation of its effect leads research on local stresses to rather deviating results ([7], [8] and [4], [29]). The Poisson's ratio is known to increase with the increasing ratio of actual to ultimate concrete stress under permanent loads. This induced us to choose simpler models assuming a fixed Poisson's ratio, remarking that a more complex framework model permits to vary this latter.

Another limitation is due to contradictions in compatibility upon applying varying mesh or to analogy inaccuracies upon reckoning with edges of oblique tetragonal units, or eventually requiring extremely fine mesh. The grid cannot adopt the reinforcement arrangement without restrictions.

Uniform mesh is advantageous because of the possible occurrence of cracks throughout the beam length, and the mesh was demonstrated ([24]) to affect the calculated value of crack width; characteristics of the tie representing the bond do not vary with the grid points.

An advantage of the framework model is the identical simulation of reinforcing or prestressing steel and of bars representing the concrete, or the ties simulating the bond.

The framework model is rather handy to consider the existing or supposed cracks in the concrete (maybe with a slight flaw in the analogy).

3. Model of elastic plane members

Determination of the displacements and internal forces of a structure seen in Fig. 1 or similar is expediently done by the deformation method, solving system of equations

$$\mathbf{K}\mathbf{u} = \mathbf{q}.$$

Elements of the unknown vectors $\mathbf{u}$ are the displacement components of the nodes, elements of the vector $\mathbf{q}$ are the components in the directions of the co-ordinate axes of the forces acting on the nodes. The coefficient of the unknown vector is the stiffness matrix $\mathbf{K}$.

For the sake of a simpler but descriptive form, let us deal with the two-dimensional problem. Consideration of cracks and reinforcement will be demonstrated in this case, generalization to the three-dimensional model will be shortly demonstrated below.

3.1 *Stiffness matrix of the plane concrete unit*

Stiffness matrix of the square grid in Fig. 1 is produced by transforming the local stiffness matrix of each bar of the model into the global reference system x, y and by compilation. To this aim, local stiffness matrices of the bar types, and in case of different nodes, elements of the stiffness matrix in, and off the main diagonal are needed.

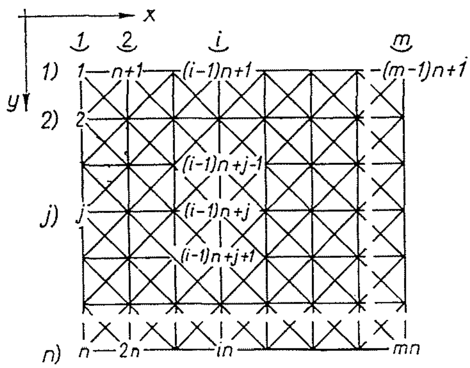

Fig. 1

3.11 Bar local stiffness matrices

Bars in directions x and y equal in length to the mesh ($l = h$) have a cross sectional area A, a modulus of elasticity E, and a stiffness $B = EA/h$, bars in the diagonal and in the secondary diagonal have a length $l_a = \sqrt{2}\, h$, a cross sectional area A_a, a modulus of elasticity E, and a stiffness $B_a = \beta B = EA_a/2\sqrt{2}h$.

Bar local stiffness matrix blocks have been compiled in Table I.

Table I

	Main diagonal blocks	Off main diagonal blocks
(v) bar in direction x	$\mathbf{K}_v = B \begin{bmatrix} 1 & 0 \\ 0 & 0 \end{bmatrix}$	$B \begin{bmatrix} -1 & 0 \\ 0 & 0 \end{bmatrix}$
(f) bar in direction y	$\mathbf{K}_f = B \begin{bmatrix} 0 & 0 \\ 0 & 1 \end{bmatrix}$	$B \begin{bmatrix} 0 & 0 \\ 0 & -1 \end{bmatrix}$
(a) bar in diagonal	$\mathbf{K}_a = \beta B \begin{bmatrix} 1 & 1 \\ 1 & 1 \end{bmatrix}$	$\beta B \begin{bmatrix} -1 & -1 \\ -1 & -1 \end{bmatrix}$
(m) bar in secondary diagonal	$\mathbf{K}_m = \beta B \begin{bmatrix} 1 & -1 \\ -1 & 1 \end{bmatrix}$	$\beta B \begin{bmatrix} -1 & 1 \\ 1 & -1 \end{bmatrix}$

3.12 Stiffness characteristics of model nodes

The case of a continuous member broken down into framework elements of mesh h is shown in Fig. 2. Thus, two adjacent elements are a double bar of stiffness B. Possible cases of node arrangement — taking simulation of cracks in item 3.14 into consideration — are seen in Fig. 3.

Each nodal variant bears the symbol of the sum of blocks in the main diagonal of local stiffness matrices of bars joining in one node. Block values have been compiled in Table II. The off-main-diagonal block of the stiffness matrix of the structure is of course zero if no bar connects nodes marked with the block symbols. Otherwise outside the main diagonal of the stiffness matrix, the secondary diagonal block of the local stiffness matrix is indicated. Cases corresponding to bars and block symbols are seen in Fig. 4, and block values in Table III.

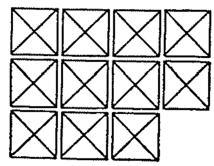

Fig. 2

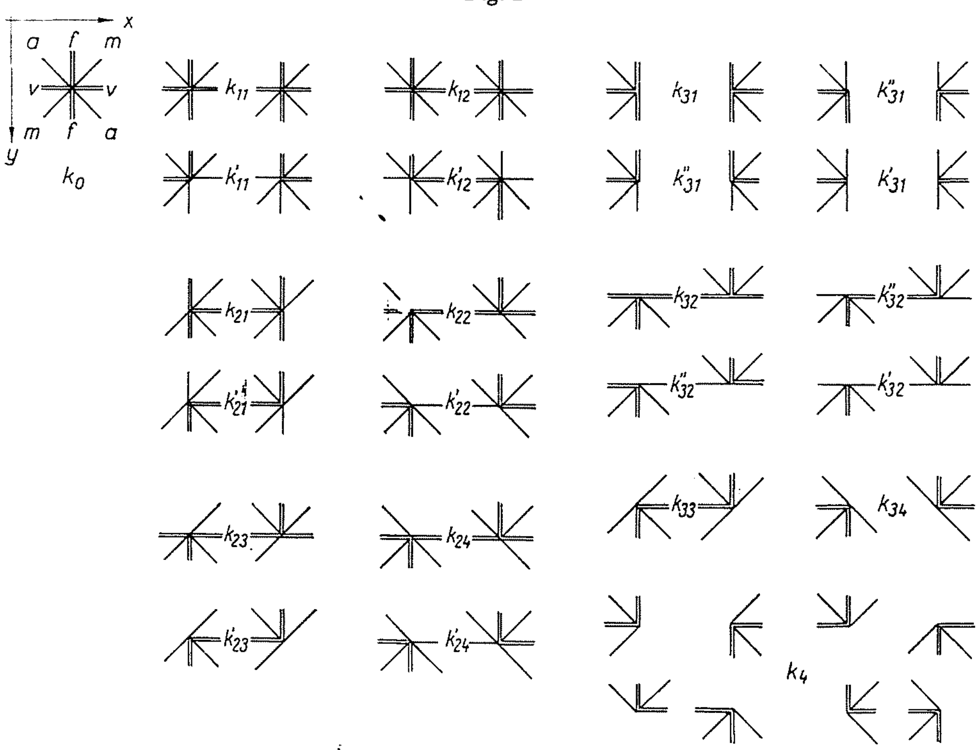

Fig. 3

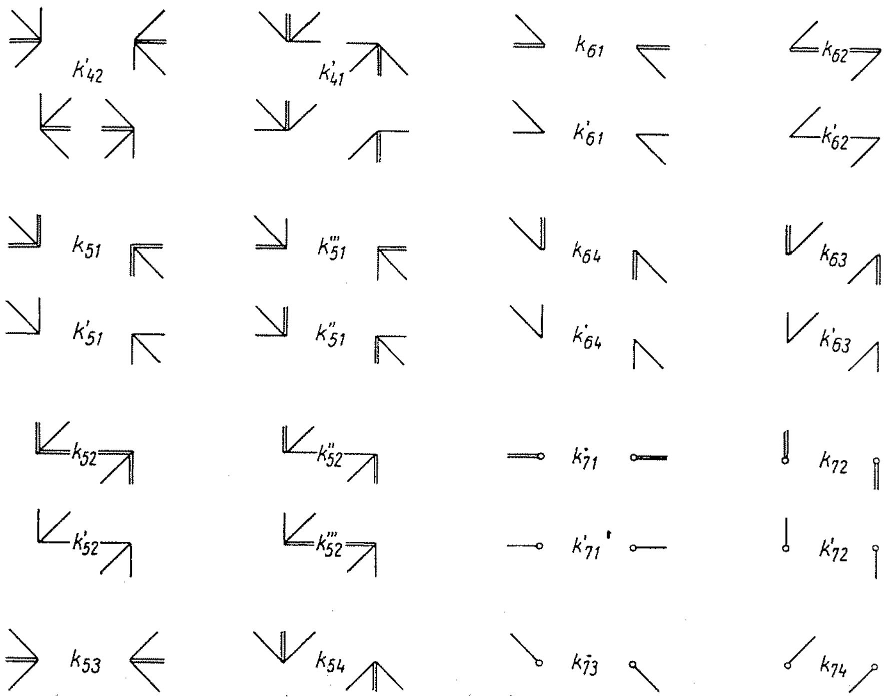

Fig. 3 (continued)

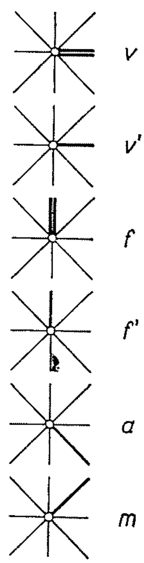

Fig. 4

Table II

Main diagonal blocks

	$\mathbf{K}_v$	$\mathbf{K}_f$	$\mathbf{K}_a$	$\mathbf{K}_m$	symbol
$\mathbf{K}_0 = 2(\mathbf{K}_v + \mathbf{K}_f + \mathbf{K}_a + \mathbf{K}_m)$	2	2	2	2	k_0
$\mathbf{K}_{11} = 2(\mathbf{K}_v + \mathbf{K}_f + \mathbf{K}_m) + \mathbf{K}_a$	2	2	1	2	k_{11}
$\mathbf{K}'_{11} = \frac{3}{2}(\mathbf{K}_v + \mathbf{K}_f) + 2\mathbf{K}_m + \mathbf{K}_a$	$\frac{3}{2}$	$\frac{3}{2}$	1	2	k'_{11}
$\mathbf{K}_{12} = 2(\mathbf{K}_v + \mathbf{K}_f + \mathbf{K}_a) + \mathbf{K}_m$	2	2	2	1	k_{12}
$\mathbf{K}'_{12} = \frac{3}{2}(\mathbf{K}_v + \mathbf{K}_f) + 2\mathbf{K}_a + \mathbf{K}_m$	$\frac{3}{2}$	$\frac{3}{2}$	2	1	k'_{12}
$\mathbf{K}_{21} = 2(\mathbf{K}_f + \mathbf{K}_m) + \mathbf{K}_v + \mathbf{K}_a$	1	2	1	2	k_{21}
$\mathbf{K}'_{21} = \frac{3}{2}\mathbf{K}_f + 2\mathbf{K}_m + \mathbf{K}_v + \mathbf{K}_a$	1	$\frac{3}{2}$	1	2	k'_{21}
$\mathbf{K}_{22} = 2(\mathbf{K}_v + \mathbf{K}_a) + \mathbf{K}_f + \mathbf{K}_m$	2	1	2	1	k_{22}
$\mathbf{K}'_{22} = \frac{3}{2}\mathbf{K}_v + 2\mathbf{K}_a + \mathbf{K}_f + \mathbf{K}_m$	$\frac{3}{2}$	1	2	1	k'_{22}
$\mathbf{K}_{23} = 2(\mathbf{K}_v + \mathbf{K}_m) + \mathbf{K}_f + \mathbf{K}_a$	2	1	1	2	k_{23}
$\mathbf{K}'_{23} = \frac{3}{2}\mathbf{K}_v + 2\mathbf{K}_m + \mathbf{K}_f + \mathbf{K}_a$	$\frac{3}{2}$	1	1	2	k'_{23}
$\mathbf{K}_{24} = 2(\mathbf{K}_v + \mathbf{K}_a) + \mathbf{K}_f + \mathbf{K}_m$	2	1	2	1	k_{24}
$\mathbf{K}'_{24} = \frac{3}{2}\mathbf{K}_v + 2\mathbf{K}_a + \mathbf{K}_f + \mathbf{K}_m$	$\frac{3}{2}$	1	2	1	k'_{24}
$\mathbf{K}_{51} = \mathbf{K}_v + \mathbf{K}_f + \mathbf{K}_a$	1	1	1	0	k_{51}
$\mathbf{K}'_{51} = \frac{1}{2}\mathbf{K}_v + \frac{1}{2}\mathbf{K}_f + \mathbf{K}_a$	$\frac{1}{2}$	$\frac{1}{2}$	1	0	k'_{51}
$K''_{51} = \frac{1}{2}\mathbf{K}_v + \mathbf{K}_f + \mathbf{K}_a$	$\frac{1}{2}$	1	1	0	k''_{51}
$\mathbf{K}'''_{51} = \mathbf{K}_v + \frac{1}{2}\mathbf{K}_f + \mathbf{K}_a$	1	$\frac{1}{2}$	1	0	k'''_{51}
$\mathbf{K}_{52} = \mathbf{K}_f + \mathbf{K}_v + \mathbf{K}_m$	1	1	0	1	k_{52}
$\mathbf{K}'_{52} = \frac{1}{2}\mathbf{K}_v + \frac{1}{2}\mathbf{K}_f + \mathbf{K}_m$	$\frac{1}{2}$	$\frac{1}{2}$	0	1	k'_{52}
$\mathbf{K}''_{52} = \mathbf{K}_f + \frac{1}{2}\mathbf{K}_v + \mathbf{K}_m$	$\frac{1}{2}$	1	0	1	k''_{52}
$\mathbf{K}'''_{52} = \mathbf{K}_v + \frac{1}{2}\mathbf{K}_f + \mathbf{K}_m$	1	$\frac{1}{2}$	0	1	k'''_{52}
$\mathbf{K}_{53} = \mathbf{K}_v + \mathbf{K}_a + \mathbf{K}_m$	1	0	1	1	k_{53}
$\mathbf{K}_{54} = \mathbf{K}_f + \mathbf{K}_a + \mathbf{K}_m$	0	1	1	1	k_{54}
$\mathbf{K}_{61} = \mathbf{K}_v + \mathbf{K}_a$	1	0	1	0	k_{61}
$\mathbf{K}'_{61} = \frac{1}{2}\mathbf{K}_v + \mathbf{K}_a$	$\frac{1}{2}$	0	1	0	k'_{61}
$\mathbf{K}_{62} = \mathbf{K}_v + \mathbf{K}_m$	1	0	0	1	k_{62}
$\mathbf{K}'_{62} = \frac{1}{2}\mathbf{K}_v + \mathbf{K}_m$	$\frac{1}{2}$	0	0	1	k'_{62}

Table II (continued)

	K_v	K_f	K_a	K_m	symbol
$K_{31} = 2K_f + K_v + K_a + K_m$	1	2	1	1	k_{31}
$K'_{31} = K_f + K_v + K_a + K_m$	1	1	1	1	k'_{31}
$K''_{31} = \frac{3}{2} K_f + K_v + K_a + K_m$	1	$\frac{3}{2}$	1	1	k''_{31}
$K_{32} = 2K_v + K_f + K_a + K_m$	2	1	1	1	k_{32}
$K'_{32} = K_v + K_f + K_a + K_m$	1	1	1	1	k'_{32}
$K''_{32} = \frac{3}{2} K_v + K_f + K_m + K_a$	$\frac{3}{2}$	1	1	1	k''_{32}
$K_{33} = K_v + K_f + 2K_m + K_a$	1	1	1	2	k_{33}
$K_{34} = K_v + K_f + 2K_a + K_m$	1	1	2	1	k_{34}
$K_4 = K_v + K_f + K_a + K_m$	1	1	1	1	k_4
$K'_{41} = K_f + \frac{1}{2} K_v + K_a + K_m$	$\frac{1}{2}$	1	1	1	k'_{41}
$K'_{42} = K_v + \frac{1}{2} K_f + K_a + K_m$	1	$\frac{1}{2}$	1	1	k'_{42}

	K_v	K_f	K_a	K_m	symbol
$K_{63} = K_f + K_m$	0	1	0	1	k_{63}
$K'_{63} = \frac{1}{2} K_f + K_m$	0	$\frac{1}{2}$	0	1	k'_{63}
$K_{64} = K_f + K_a$	0	1	1	0	k_{64}
$K'_{64} = \frac{1}{2} K_f + K_a$	0	$\frac{1}{2}$	1	0	k'_{64}
$K_{71} = K_v$	1	0	0	0	k_{71}
$K'_{71} = \frac{1}{2} K_v$	$\frac{1}{2}$	0	0	0	k'_{71}
$K_{72} = K_f$	0	1	0	0	k_{72}
$K'_{72} = \frac{1}{2} K_f$	0	$\frac{1}{2}$	0	0	k'_{72}
$K_{73} = K_a$	0	0	1	0	k_{73}
$K_{74} = K_m$	0	0	0	1	k_{74}

Table II (continued)

$k_0 = B\begin{bmatrix} 2+4\beta & 0 \\ 0 & 2+4\beta \end{bmatrix}$	$k_{32} = B\begin{bmatrix} 2+2\beta & 0 \\ 0 & 1+2\beta \end{bmatrix}$	$k_{53} = B\begin{bmatrix} 1+2\beta & 0 \\ 0 & 2\beta \end{bmatrix}$
$k_{11} = B\begin{bmatrix} 2+3\beta & -\beta \\ -\beta & 2+3\beta \end{bmatrix}$	$k'_{32} = B\begin{bmatrix} 1+2\beta & 0 \\ 0 & 1+2\beta \end{bmatrix}$	$k_{54} = B\begin{bmatrix} 2\beta & 0 \\ 0 & 1+2\beta \end{bmatrix}$
$k'_{11} = B\begin{bmatrix} 3/2+3\beta & -\beta \\ -\beta & 3/2+3\beta \end{bmatrix}$	$k''_{32} = B\begin{bmatrix} 3/2+2\beta & 0 \\ 0 & 1+2\beta \end{bmatrix}$	$k_{61} = B\begin{bmatrix} 1+\beta & \beta \\ \beta & \beta \end{bmatrix}$
$k_{12} = B\begin{bmatrix} 2+3\beta & \beta \\ \beta & 2+3\beta \end{bmatrix}$	$k_{33} = B\begin{bmatrix} 1+3\beta & -\beta \\ -\beta & 1+3\beta \end{bmatrix}$	$k'_{61} = B\begin{bmatrix} 1/2+\beta & \beta \\ \beta & \beta \end{bmatrix}$
$k'_{12} = B\begin{bmatrix} 3/2+3\beta & \beta \\ \beta & 3/2+3\beta \end{bmatrix}$	$k_{34} = B\begin{bmatrix} 1+3\beta & \beta \\ \beta & 1+3\beta \end{bmatrix}$	$k_{62} = B\begin{bmatrix} 1+\beta & -\beta \\ -\beta & \beta \end{bmatrix}$
$k_{21} = B\begin{bmatrix} 1+3\beta & \beta-\beta \\ -\beta & 2+3\beta \end{bmatrix}$	$k_4 = B\begin{bmatrix} 1+2\beta & 0 \\ 0 & 1+2\beta \end{bmatrix}$	$k'_{62} = B\begin{bmatrix} 1/2+\beta & -\beta \\ -\beta & \beta \end{bmatrix}$
$k'_{21} = B\begin{bmatrix} 1+3\beta & -\beta \\ -\beta & 3/2+3\beta \end{bmatrix}$	$k'_{41} = B\begin{bmatrix} 1/2+2\beta & 0 \\ 0 & 1+2\beta \end{bmatrix}$	$k_{63} = B\begin{bmatrix} \beta & -\beta \\ -\beta & 1+\beta \end{bmatrix}$
$k_{22} = B\begin{bmatrix} 2+3\beta & \beta \\ \beta & 1+3\beta \end{bmatrix}$	$k'_{42} = B\begin{bmatrix} 1+2\beta & 0 \\ 0 & 1/2+2\beta \end{bmatrix}$	$k'_{63} = B\begin{bmatrix} \beta & -\beta \\ -\beta & 1/2+\beta \end{bmatrix}$
$k'_{22} = B\begin{bmatrix} 3/2+3\beta & \beta \\ \beta & 1+3\beta \end{bmatrix}$	$k_{51} = B\begin{bmatrix} 1+\beta & \beta \\ \beta & 1+\beta \end{bmatrix}$	$k_{64} = B\begin{bmatrix} \beta & \beta \\ \beta & 1+\beta \end{bmatrix}$
$k_{23} = B\begin{bmatrix} 2+3\beta & -\beta \\ -\beta & 1+3\beta \end{bmatrix}$	$k'_{51} = B\begin{bmatrix} 1/2+\beta & \beta \\ \beta & 1/2+\beta \end{bmatrix}$	$k'_{64} = B\begin{bmatrix} \beta & \beta \\ \beta & 1/2+\beta \end{bmatrix}$
$k'_{23} = B\begin{bmatrix} 3/2+3\beta & -\beta \\ -\beta & 1+3\beta \end{bmatrix}$	$k''_{51} = B\begin{bmatrix} 1/2+\beta & \beta \\ \beta & 1+\beta \end{bmatrix}$	$k_{71} = B\begin{bmatrix} 1 & 0 \\ 0 & 0 \end{bmatrix}$
$k_{24} = B\begin{bmatrix} 2+3\beta & \beta \\ \beta & 1+3\beta \end{bmatrix}$	$k'''_{51} = B\begin{bmatrix} 1+\beta & \beta \\ \beta & 1/2+\beta \end{bmatrix}$	$k'_{71} = B\begin{bmatrix} 1/2 & 0 \\ 0 & 0 \end{bmatrix}$
$k'_{24} = B\begin{bmatrix} 3/2+3\beta & \beta \\ \beta & 1+3\beta \end{bmatrix}$	$k_{52} = B\begin{bmatrix} 1+\beta & -\beta \\ -\beta & 1+\beta \end{bmatrix}$	$k_{72} = B\begin{bmatrix} 0 & 0 \\ 0 & 1 \end{bmatrix}$
$k_{31} = B\begin{bmatrix} 1+2\beta & 0 \\ 0 & 2+2\beta \end{bmatrix}$	$k'_{52} = B\begin{bmatrix} 1/2+\beta & -\beta \\ -\beta & 1/2+\beta \end{bmatrix}$	$k'_{72} = B\begin{bmatrix} 0 & 0 \\ 0 & 1/2 \end{bmatrix}$
$k'_{31} = B\begin{bmatrix} 1+2\beta & 0 \\ 0 & 1+2\beta \end{bmatrix}$	$k''_{52} = B\begin{bmatrix} 1/2+\beta & -\beta \\ -\beta & 1+\beta \end{bmatrix}$	$k_{73} = B\begin{bmatrix} \beta & \beta \\ \beta & \beta \end{bmatrix}$
$k''_{31} = B\begin{bmatrix} 1+2\beta & 0 \\ 0 & 3/2+2\beta \end{bmatrix}$	$k'''_{52} = B\begin{bmatrix} 1+\beta & -\beta \\ -\beta & 1/2+\beta \end{bmatrix}$	$k_{74} = B\begin{bmatrix} \beta & -\beta \\ -\beta & \beta \end{bmatrix}$

Table III

Off main diagonal blocks

$$\mathbf{V} = B\begin{bmatrix} -1 & 0 \\ 0 & 0 \end{bmatrix} \quad \text{symbol } v$$

$$\mathbf{V}' = B\begin{bmatrix} -1/2 & 0 \\ 0 & 0 \end{bmatrix} \quad \text{symbol } v'$$

$$\mathbf{F} = B\begin{bmatrix} 0 & 0 \\ 0 & -1 \end{bmatrix} \quad \text{symbol } f$$

$$\mathbf{F}' = B\begin{bmatrix} 0 & 0 \\ 0 & -1/2 \end{bmatrix} \quad \text{symbol } f'$$

$$\mathbf{A} = B\begin{bmatrix} -\beta & -\beta \\ -\beta & -\beta \end{bmatrix} \quad \text{symbol } a$$

$$\mathbf{M} = B\begin{bmatrix} -\beta & \beta \\ \beta & -\beta \end{bmatrix} \quad \text{symbol } m$$

3.13 Stiffness of a square continuum model

$4\ (m \times n)^2$ size stiffness matrix of a model with $m \times n$ nodes seen in Fig. 1 can be written as

$$\mathbf{K} = \begin{bmatrix} \mathbf{A}^{I} & \mathbf{L} & & & \\ \mathbf{L}^{T} & \mathbf{A} & \mathbf{L} & & \\ & \cdot & \cdot & \cdot & \\ & & \cdot & \cdot & \cdot \\ & & \mathbf{L}^{T} & \mathbf{A} & \mathbf{L} \\ & & & \mathbf{L}^{T} & \mathbf{A}^{II} \end{bmatrix}, \quad (mn$$

where blocks of size $4\ n^2$ in the diagonal are:

$$\mathbf{A}^{I} = \begin{bmatrix} k'_{51} & f' & & & \\ f' & k'_{31} & f'' & & \\ & \cdot & \cdot & \cdot & \\ & & \cdot & \cdot & \cdot \\ & & f' & k'_{31} & f' \\ & & & f' & k'_{52} \end{bmatrix} (n, \qquad \mathbf{A} = \begin{bmatrix} k'_{32} & f & & & \\ f' & k_0 & f & & \\ & \cdot & \cdot & \cdot & \\ & & \cdot & \cdot & \cdot \\ & & f & k_0 & f \\ & & & f & k'_{32} \end{bmatrix} (n,$$

$$\mathbf{A}^{II} = \begin{bmatrix} k''_{52} & f' & & & \\ f' & k'_{31} & f & & \\ & \cdot & \cdot & \cdot & \\ & & \cdot & \cdot & \cdot \\ & & f' & k'_{31} & f' \\ & & & f' & k'_{51} \end{bmatrix} (n.$$

Accordingly, matrix $\mathbf{A}^{II}$ is produced by mirroring matrix $\mathbf{A}^{I}$ onto the secondary diagonal, but only the 2×2 block has to be mirrored, without the contained elements.

Matrices in the codiagonal of $\mathbf{K}$ are:

$$\mathbf{L} = \begin{bmatrix} v' & a & & & & \\ m & v & a & & & \\ & \cdot & \cdot & \cdot & & \\ & & \cdot & \cdot & \cdot & \\ & & & \cdot & \cdot & \cdot \\ & & & m & v & a \\ & & & & m & v' \end{bmatrix} (n$$

of size $4\,m^2$, and their transpose $\mathbf{L}$.

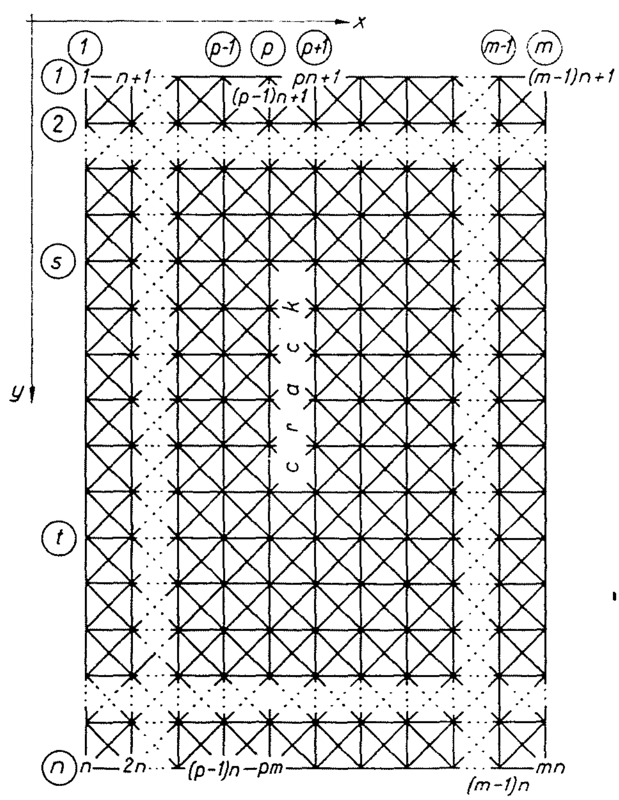

Fig. 5

3.14 Stiffness matrix of elements with an arbitrary boundary or with cracks

Stiffness matrix of a model of a non-tetragonal unit with sides parallel to axes x or y can be written to the sense. For sides other than parallel to the co-ordinate axes, the skew edges may be replaced by stepped lines, or — to the detriment of accuracy of analogy — the framework elements may be slightly off-quadratic.

In the model there are two ways of reckoning with a crack along a given line. The first is by omitting the stiffness of bars crossed by the crack. This method is exempt of topology difficulties, namely there are as many elements in the stiffness matrix as in the model of an uncracked structure of the identical boundaries. Analogy is made incomplete by cuts, but this simulation of cracks reckons with the subsistence of the unit in spite of the crack and the possibility of forces acting parallel with the crack.

The crack can also be simulated by assuming it to lie along the boundary of units consisting of rectangular booms and diagonals, more exactly, the double bars split along the length. This second way is less disturbing to the analogy. Its stiffness matrix is made, however, more complicated by requiring the assumption of separate nodes at two end points of the crack, increasing the number of unknowns. Order of the stiffness matrix is affected by the variation of the crack shape and length, and this alternative is laboured for assuming different crack patterns, or even crack propagation. Thus, only the first method will be expounded below.

3.141 *Vertical crack*

Assume crack pattern according to Fig. 5, with the pertaining stiffness matrix:

$$
\mathbf{K}_{rf} = \begin{bmatrix}
\mathbf{A}^{I} & \mathbf{L} & & & & & & & \\
\mathbf{L}^{T} & \mathbf{A} & \mathbf{L} & & & & & & \\
 & \ddots & \ddots & \ddots & & & & & \\
 & & \mathbf{L}^{T} & \mathbf{A} & \mathbf{L} & & & & \\
 & & & \mathbf{L}^{T} & \mathbf{A}_{rf1} & \mathbf{L}_{rf} & & & \\
 & & & & \mathbf{L}_{rf}^{T} & \mathbf{A}_{rf2} & \mathbf{L} & & \\
 & & & & & \mathbf{L}^{T} & \mathbf{A} & \mathbf{L} & \\
 & & & & & & \ddots & \ddots & \ddots \\
 & & & & & & \mathbf{L}^{T} & \mathbf{A} & \mathbf{L} \\
 & & & & & & & \mathbf{L}^{T} & \mathbf{A}^{II}
\end{bmatrix}
\begin{array}{l}
(1 \\ (2 \\ \\ \\ (p \\ (p+1 \\ \\ \\ \\ (m
\end{array}
$$

In general:

$$
\mathbf{A}_{rf1} = \left[\begin{array}{ccccccccccccc}
k'_{32} & f & & & & & & & & & & & \\
f & k_0 & f & & & & & & & & & & \\
 & f & k_0 & f & & & & & & & & & \\
 & & f & k_{11} & f & & & & & & & & \\
 & & & f & k_{31} & f & & & & & & & \\
 & & & & f & k_{31} & f & & & & & & \\
 & & & & & \ddots & \ddots & \ddots & & & & & \\
 & & & & & & f & k_{31} & f & & & & \\
 & & & & & & & f & k_{31} & f & & & \\
 & & & & & & & & f & k_{12} & f & & \\
 & & & & & & & & & f & k_0 & f & \\
 & & & & & & & & & & f & k_0 & f \\
 & & & & & & & & & & & f & k'_{32}
\end{array}\right]
\begin{array}{l}
((p-1)n+1 \\ \\ \\ ((p-1)n+s \\ ((p-1)n+s+1 \\ \\ (p) \\ \\ ((p-1)n+t-1 \\ ((p-1)n+t \\ \\ \\ (pn
\end{array}
$$

Block $\mathbf{A}_{rf2}$ is produced by mirroring the modified block part marked by dash line in block $\mathbf{A}_{rf1}$ onto the secondary diagonal, where blocks size 2×2 are not mirrored onto their own secondary diagonals.

$\mathbf{L}_{rf}$ in the codiagonal of the stiffness matrix becomes

$$
\mathbf{L}_{rf} = \left[\begin{array}{cccccccccc}
\nu' & a & & & & & & & & \\
m & \nu & a & & & & & & & \\
 & m & \nu & a & & & & & & \\
 & & m & \nu & & & & & & \\
 & & & & & & & & & \\
 & & & & & & & & & \\
 & & & & & & & & & \\
 & & & & & & \nu & a & & \\
 & & & & & & m & \nu & a & \\
 & & & & & & & m & \nu & a \\
 & & & & & & & & m & \nu'
\end{array}\right]
\begin{array}{l}
((p-1)n+1 \\ \\ \\ ((p-1)n+s \\ ((p-1)n+s+1 \\ (p) \\ ((p-1)n+t-1 \\ ((p-1)n+t \\ \\ \\ (pn
\end{array}
$$

$\mathbf{L}^T_{rf}$ being its transpose.

A crack starting from the lower edge has blocks of size $2 \times 2 \times n \times n$ of the form:

$$
A_{rf1} = \begin{array}{c}
\left[\begin{array}{cccccccccc}
k_{32} & f & & & & & & & & \\
f & k_0 & f & & & & & & & \\
 & f & k_0 & f & & & & & & \\
 & & f & k_{11} & f & & & & & \\
 & & & f & k_{31} & f & & & & \\
 & & & & f & k_{31} & f & & & \\
 & & & & & \ddots & \ddots & \ddots & & \\
 & & & & & & f & k_{31} & f & \\
 & & & & & & & f & k_{31} & f \\
 & & & & & & & & f & k''_{51}
\end{array}\right]
\end{array}
\begin{array}{l}
((p-1)n+1 \\
\\
\\
((p-1)n+s \\
((p-1)n+s+1 \\
\\
(p) \\
\\
\\
(pn
\end{array}
$$

and also $\mathbf{A}_{rf2}$, $\mathbf{L}_{rf}$ and $\mathbf{L}_{rf}^T$ are modified accordingly.

3.142 Horizontal crack

Stiffness matrix of a member crossed by a horizontal crack (Fig. 6) is of the form:

$$
K_{rv} = \left[\begin{array}{cccccccccc}
A^I & L & & & & & & & & \\
L^T & A & L & & & & & & & \\
 & L^T & A & L & & & & & & \\
 & & L^T & A_{rv1} & L_{rv} & & & & & \\
 & & & L_{rv}^T & A_{rv2} & L_{rv} & & & & \\
 & & & & \ddots & \ddots & \ddots & & & \\
 & & & & & \ddots & \ddots & \ddots & & \\
 & & & & & L_{rv}^T & A_{rv2} & L_{rv} & & \\
 & & & & & & L_{rv}^T & A_{rv3} & L & \\
 & & & & & & & L^T & A & L \\
 & & & & & & & & L^T \;\; A & L \\
 & & & & & & & & L^T & A^{II}
\end{array}\right]
\begin{array}{l}
(1 \\
(2 \\
\\
(s \\
(s+1 \\
(s+2 \\
(t-2 \\
(t-1 \\
(t \\
\\
(m-1 \\
(m
\end{array}
$$

where

$$
\mathbf{A}_{rv1} = \begin{array}{cl}
\left[\begin{array}{ccccccccccc}
k'_{32} & f & & & & & & & & & \\
f & k_0 & f & & & & & & & & \\
 & \ddots & \ddots & \ddots & & & & & & & \\
 & & f & k_0 & f & & & & & & \\
 & & & f & k_{11} & f & & & & & \\
 & & & & f & k_{12} & f & & & & \\
 & & & & & f & k_0 & f & & & \\
 & & & & & & \ddots & \ddots & \ddots & & \\
 & & & & & & & \ddots & \ddots & \ddots & \\
 & & & & & & & & f & k_0 & f \\
 & & & & & & & & & f & k'_{32}
\end{array}\right] &
\begin{array}{l}
((s-1)n+1 \\
((s-1)n+2 \\
\\
\\
((s-1)n+p \\
((s-1)n+p+1 \\
\\
s \\
\\
(sn-1 \\
(sn
\end{array}
\end{array}
$$

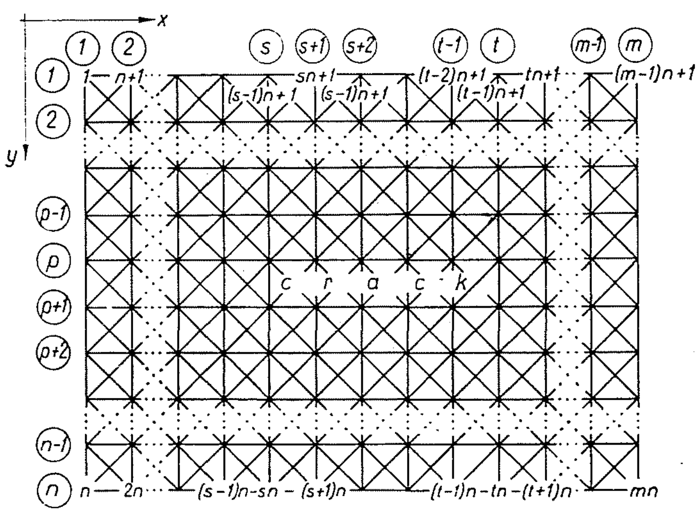

Fig. 6

$$
A_{rv2} = \left[\begin{array}{cccccccccc}
k'_{32} & f & & & & & & & & \\
f & k_0 & f & & & & & & & \\
 & \ddots & \ddots & \ddots & & & & & & \\
 & & f & k_0 & f & & & & & \\
 & & & f & k_{32} & 0 & & & & \\
 & & & & 0 & k_{32} & f & & & \\
 & & & & & f & k_0 & f & & \\
 & & & & & & \ddots & \ddots & \ddots & \\
 & & & & & & & f & k_0 & f \\
 & & & & & & & & f & k'_{32}
\end{array}\right]
\begin{array}{l}
(sn+1 \\
(sn+2 \\
 \\
 \\
(sn+p \\
(sn+p+1 \\
 \\
s+1 \\
((s+1)n-1 \\
((s+1)n
\end{array}
$$

$$
A_{rv3} = \left[\begin{array}{cccccccccc}
k'_{32} & f & & & & & & & & \\
f & k_0 & f & & & & & & & \\
 & \ddots & \ddots & \ddots & & & & & & \\
 & & f & k_0 & f & & & & & \\
 & & & f & k_{12} & f & & & & \\
 & & & & f & k_{11} & f & & & \\
 & & & & & f & k_0 & f & & \\
 & & & & & & \ddots & \ddots & \ddots & \\
 & & & & & & & f & k_0 & f \\
 & & & & & & & & f & k'_{32}
\end{array}\right]
\begin{array}{l}
((t-1)n+1 \\
((t-1)n+2 \\
 \\
 \\
((t-1)n+p \\
((t-1)n+p+1 \\
 \\
t \\
(tn-1 \\
(tn
\end{array}
$$

$$
\mathbf{L}_{rv} = \left[\begin{array}{cccccccccc}
\nu' & a & & & & & & & & \\
m & \nu & a & & & & & & & \\
 & \ddots & \ddots & \ddots & & & & & & \\
 & & m & \nu & a & & & & & \\
 & & & m & \nu & 0 & & & & \\
 & & & & 0 & \nu & a & & & \\
 & & & & & m & \nu & a & & \\
 & & & & & & \ddots & \ddots & \ddots & \\
 & & & & & & & m & \nu & a \\
 & & & & & & & & m & \nu'
\end{array}\right]
\begin{array}{l}
((t-1)n+1 \\
((t-1)n+2 \\
\\
\\
((t-1)n+p \\
((t-1)n+p+1 \\
\\
t \\
(tn-1 \\
(tn
\end{array}
$$

In case of a crack attaining the left-side vertical edge, there is a stiffness matrix

$$
\mathbf{K}'_{rv} = \left[\begin{array}{cccccccc}
\mathbf{A}^{I} & \mathbf{L}_{rv} & & & & & & \\
\mathbf{L}_{rv}^{T} & \mathbf{A}_{rv2} & \mathbf{L}_{rv} & & & & & \\
 & \ddots & \ddots & \ddots & & & & \\
 & & \mathbf{L}_{rv}^{T} & \mathbf{A}_{rv2} & \mathbf{L}_{rv} & & & \\
 & & & \mathbf{L}_{rv}^{T} & \mathbf{A}_{rv3} & & & \\
 & & & & \mathbf{L}^{T} & \mathbf{A} & \mathbf{L} & \\
 & & & & & \mathbf{L}^{T} & \mathbf{A} & \mathbf{L} \\
 & & & & & & \mathbf{L}^{T} & \mathbf{A}^{II}
\end{array}\right]
\begin{array}{l}
(1 \\
(2 \\
(t-2 \\
(t-1 \\
(t \\
\\
(m-1 \\
(m
\end{array}
$$

where

$$
\mathbf{A}^I_{rv} = \begin{bmatrix}
k'_{51} & f' \\
f' & k'_{31} & f' \\
& \ddots & \ddots & \ddots \\
&& f' & k'_{31} & f' \\
&&& f' & k'''_{52} & 0 \\
&&&& 0 & k'''_{51} & f' \\
&&&&& f' & k'_{31} & f' \\
&&&&&& \ddots & \ddots & \ddots \\
&&&&&&& f' & k'_{31} & f' \\
&&&&&&&& f' & k'_{52}
\end{bmatrix}
\begin{matrix} (1 \\ (2 \\ \\ \\ (p \\ (p+1 \\ \\ 1 \\ (n-1 \\ (n \end{matrix}
$$

and $\mathbf{A}_{rv2}$, $\mathbf{A}_{rv3}$ and $\mathbf{L}_{rv}$ are as before. Stiffness matrix for a crack reaching to the right-side extreme fibre is written accordingly.

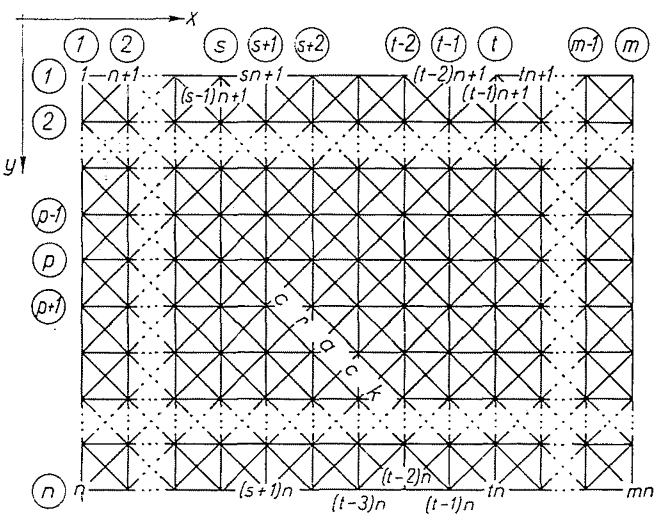

Fig. 7

3.143 Skew cracks

The problem of simulating a concrete unit with cracks is made more difficult in case of skew cracks. In case of a crack of arbitrary shape, the stiffness matrix can be written by omitting the stiffness of cut bars. For a crack crossing a node, by definition it has to be decided, the bars of which side have to be cut.

Blocks of the tri-diagonal hypermatrix exhibit a certain periodicity, not to be considered in details.

For a crack at 45° starting from the bottom fibre (Fig. 7) the stiffness matrix becomes:

$$K_{r45^\circ} = \left[\begin{array}{ccccccccccccc}
A^I & L & & & & & & & & & & & \\
L^T & A & L & & & & & & & & & & \\
 & \ddots & \ddots & \ddots & & & & & & & & & \\
 & & L^T & A & L & & & & & & & & \\
 & & & L^T & A_1 & L_1 & & & & & & & \\
 & & & & L_1^T & A_2 & L_2 & & & & & & \\
 & & & & & L_2^T & A_3 & L_3 & & & & & \\
 & & & & & & L_3^T & A_4 & L_4 & & & & \\
 & & & & & & & L_4^T & A_5 & L & & & \\
 & & & & & & & & L^T & A & L & & \\
 & & & & & & & & & \ddots & \ddots & \ddots & \\
 & & & & & & & & & & L^T & A & L \\
 & & & & & & & & & & & L^T & A^{II}
\end{array}\right]
\begin{array}{l}
(1 \\ (2 \\ \\ \\ (s \\ \\ \\ \\ (t \\ \\ \\ (m-1 \\ (m
\end{array}$$

The block shapes are indicated by the following details (involving the main diagonal):

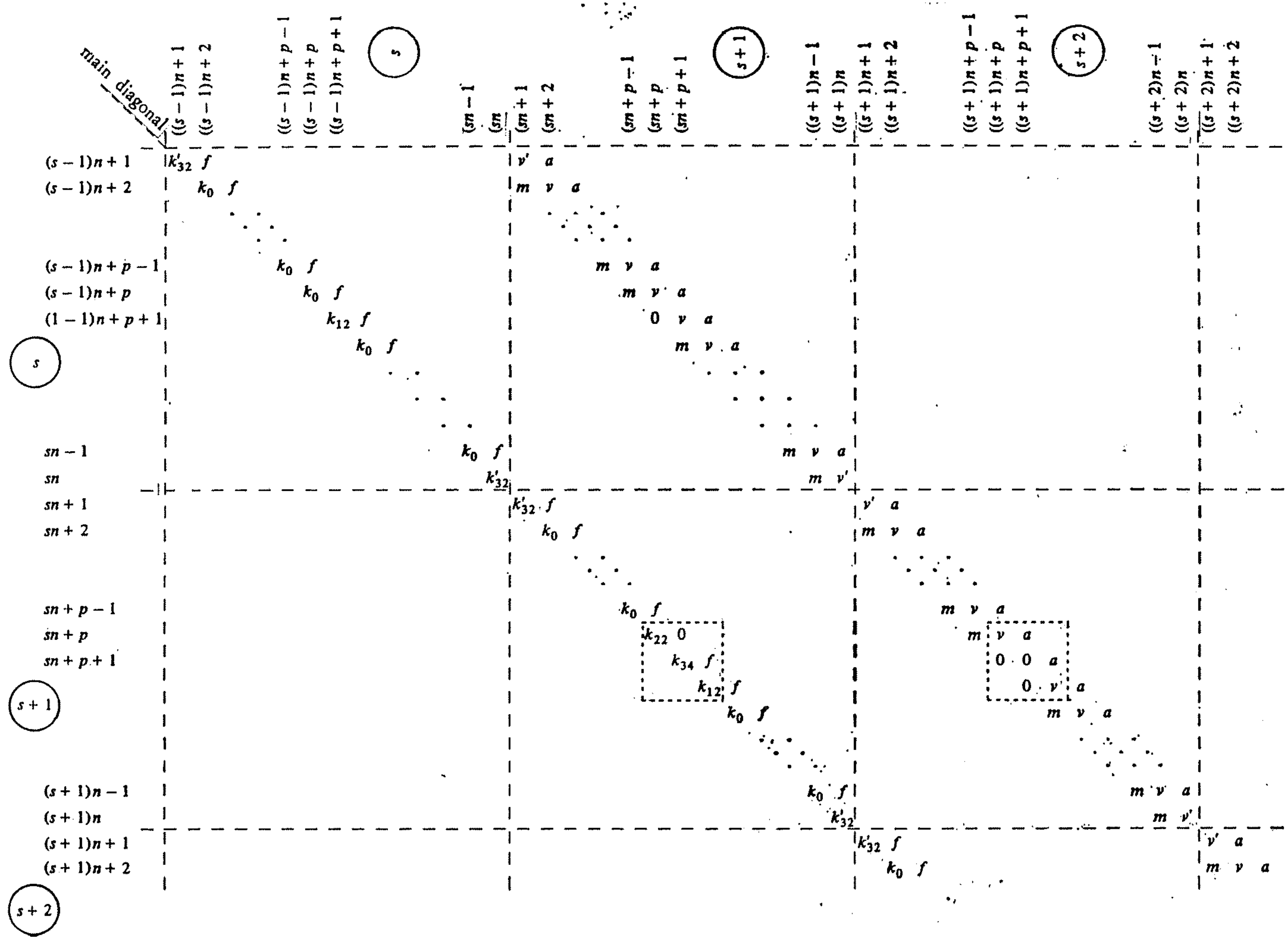
main diagonal
((s − 1)n + 1
((s − 1)n + 2
((s − 1)n + p − 1
((s − 1)n + p
((s − 1)n + p + 1
s
(sn − 1
(sn
(sn + 1
(sn + 2
(sn + p − 1
(sn + p
(sn + p + 1
s + 1
((s + 1)n − 1
((s + 1)n
((s + 1)n + 1
((s + 1)n + 2
((s + 1)n + p − 1
((s + 1)n + p
((s + 1)n + p + 1
s + 2
((s + 2)n − 1
((s + 2)n
((s + 2)n + 1
((s + 2)n + 2
(s − 1)n + 1
(s − 1)n + 2
(s − 1)n + p − 1
(s − 1)n + p
(1 − 1)n + p + 1
s
sn − 1
sn
sn + 1
sn + 2
sn + p − 1
sn + p
sn + p + 1
s + 1
(s + 1)n − 1
(s + 1)n
(s + 1)n + 1
(s + 1)n + 2
s + 2

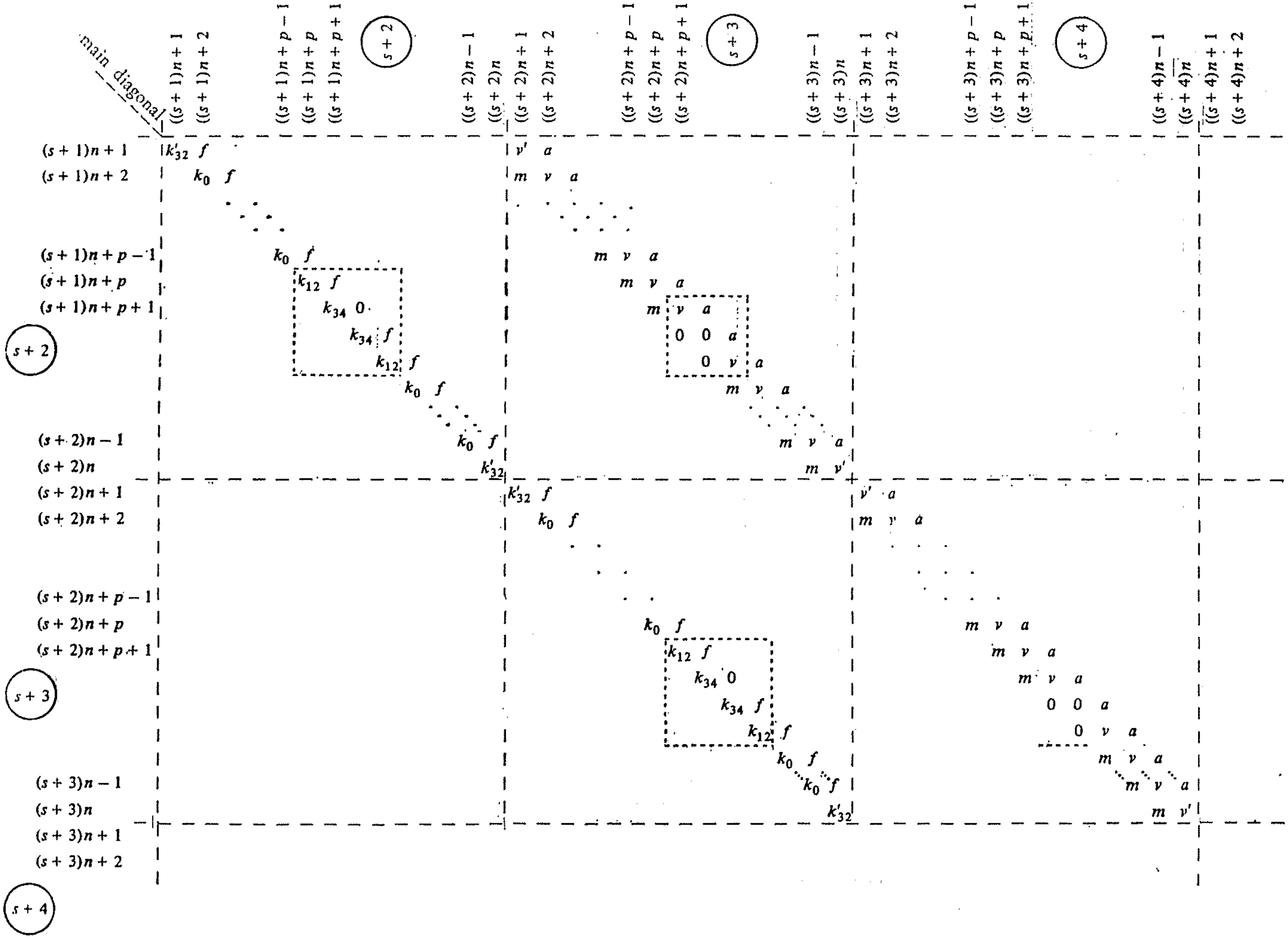
main diagonal
((s + 1)n + 1
((s + 1)n + 2
((s + 1)n + p − 1
((s + 1)n + p
((s + 1)n + p + 1
s + 2
((s + 2)n − 1
((s + 2)n
((s + 2)n + 1
((s + 2)n + 2
((s + 2)n + p − 1
((s + 2)n + p
((s + 2)n + p + 1
s + 3
((s + 3)n − 1
((s + 3)n
((s + 3)n + 1
((s + 3)n + 2
((s + 3)n + p − 1
((s + 3)n + p
((s + 3)n + p + 1
s + 4
((s + 4)n − 1
((s + 4)n
((s + 4)n + 1
((s + 4)n + 2
(s + 1)n + 1
(s + 1)n + 2
(s + 1)n + p − 1
(s + 1)n + p
(s + 1)n + p + 1
s + 2
(s + 2)n − 1
(s + 2)n
(s + 2)n + 1
(s + 2)n + 2
(s + 2)n + p − 1
(s + 2)n + p
(s + 2)n + p + 1
s + 3
(s + 3)n − 1
(s + 3)n
(s + 3)n + 1
(s + 3)n + 2
s + 4

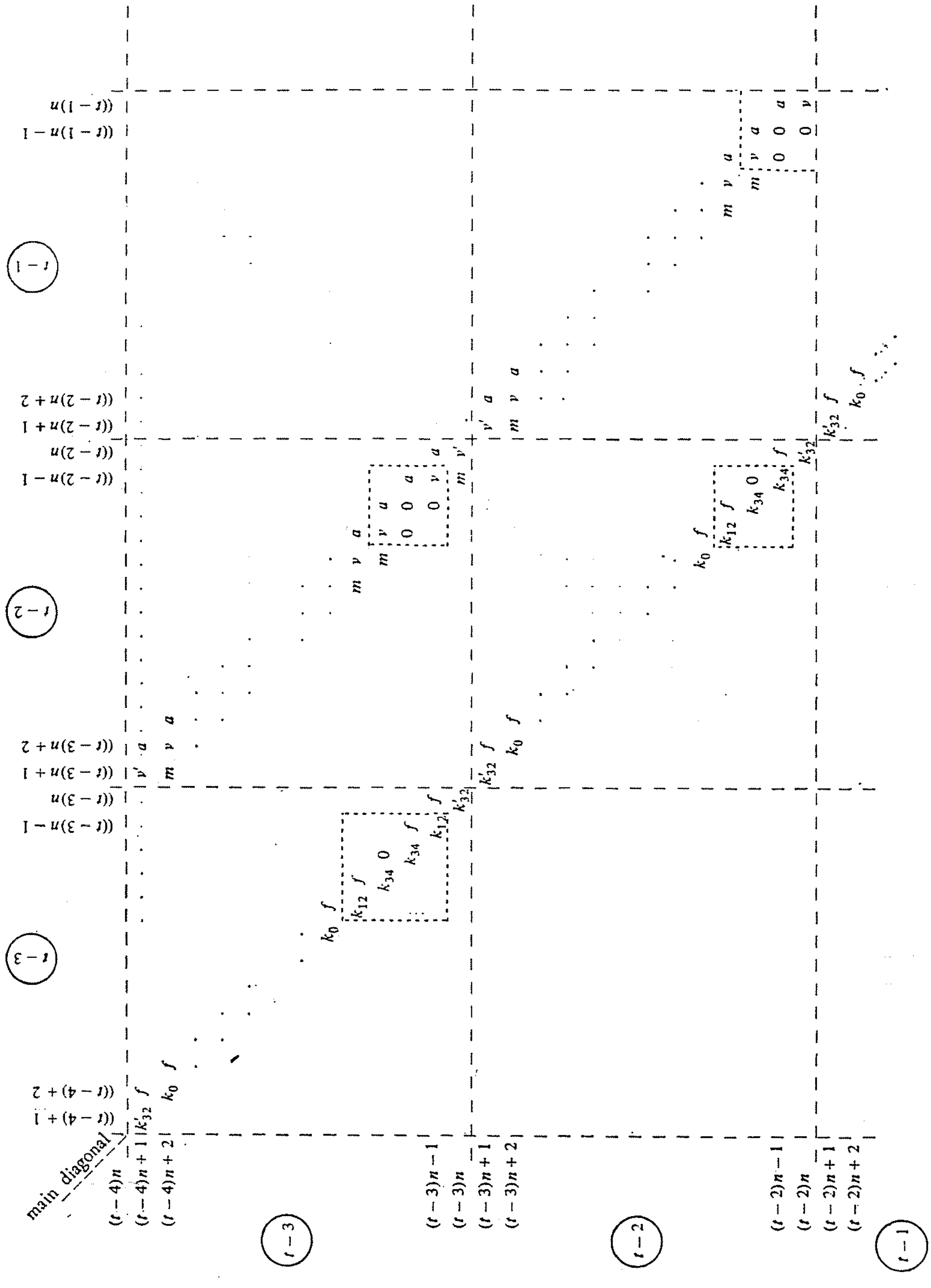
main diagonal
(t − 4)n
(t − 4)n + 1
(t − 4)n + 2
(t − 3)n − 1
(t − 3)n
(t − 3)n + 1
(t − 3)n + 2
(t − 2)n − 1
(t − 2)n
(t − 2)n + 1
(t − 2)n + 2
t − 3
t − 2
t − 1

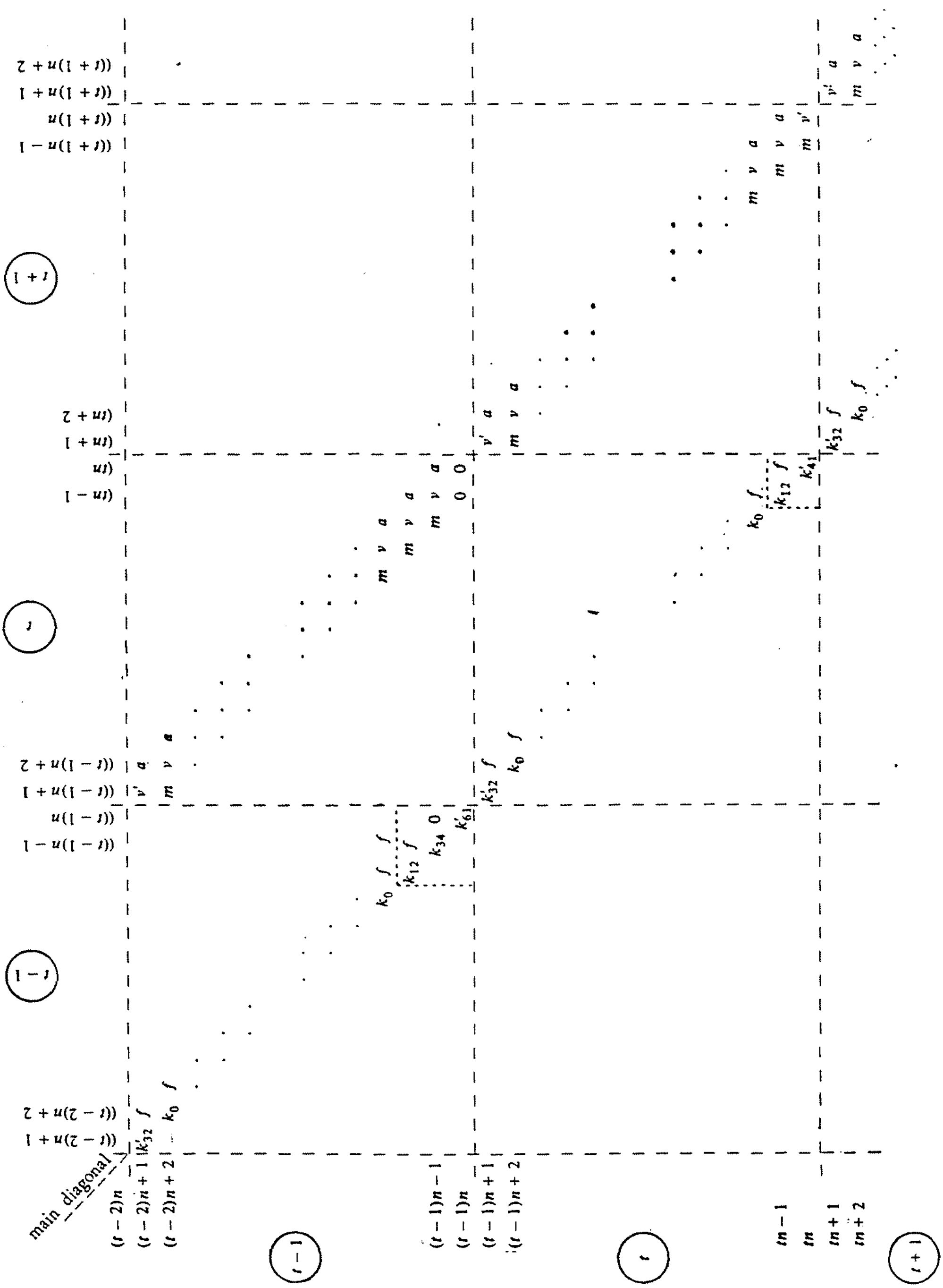
main diagonal

3.2 *Reckoning with the reinforcement in the model stiffness*

Any two nodes of the investigated framework model can be connected by a reinforcement, but here only reinforcement parallel to the co-ordinate axes will be considered (Fig. 8).

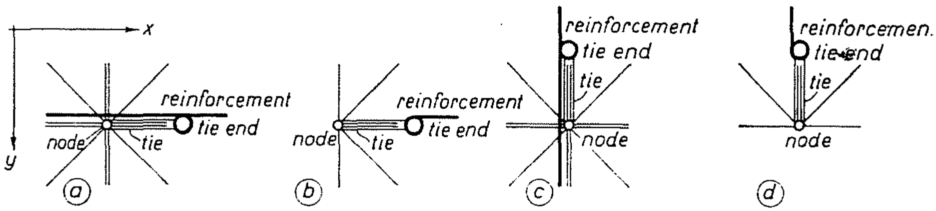

Fig. 8

3.21 Reinforcement stiffness

Let $E_{\blacksquare}$ be the modulus of elasticity of the reinforcing steel; let $A_{\blacksquare v}$ and $A_{\blacksquare f}$ be the cross sectional areas of the horizontal and vertical reinforcement, resp., and h the mesh, then stiffnesses are:

$$B_{\blacksquare v} = \frac{E_{\blacksquare} A_{\blacksquare v}}{h}\,; \qquad B_{\blacksquare f} = \frac{E_{\blacksquare} A_{\blacksquare f}}{h}\,.$$

The additive element in the main diagonal blocks of the stiffness matrix of the model, for horizontal or vertical reinforcement ending in the node is

$$B_{\blacksquare v}\begin{bmatrix} 1 & 0 \\ 0 & 0 \end{bmatrix}, \quad \text{symbol } k_{0\blacksquare v} \quad \text{and} \quad B_{\blacksquare f}\begin{bmatrix} 0 & 0 \\ 0 & 1 \end{bmatrix}, \quad \text{symbol } k_{0\blacksquare f},$$

the double is valid for reinforcements continuous over the node. The additive element off the main diagonal, for horizontal or vertical reinforcement is

$$B_{\blacksquare v}\begin{bmatrix} -1 & 0 \\ 0 & 0 \end{bmatrix}, \quad \text{symbol } v_{\blacksquare} \quad \text{and} \quad B_{\blacksquare f}\begin{bmatrix} 0 & 0 \\ 0 & -1 \end{bmatrix}, \quad \text{symbol } f_{\blacksquare}.$$

3.22 Reckoning with the bond

Assuming the bond to be given by the relationship between the relative displacement and the bond force ([23], [20]), the bond can be simulated by ties with given mechanical characteristics inserted between the nodes of finite models of the concrete and the reinforcement. For a linear relationship ([9], [19]), the bond will appear in analogy to the framework model elements in the stiffness matrix.

The ties of the horizontal and vertical steel may be affected by stiffness characteristics B_{kv} and B_{kf}, respectively. Of course, modulus of elasticity, cross sectional area and tie length can be fictitiously assigned. Knowing the relationship

$$\tau_k = \frac{t_k}{p_d} = \frac{\Delta u}{\lambda p_d} = \frac{\Delta u}{\Lambda}$$

between the bond shear stress τ_k and the relative displacement Δu, where t_k is the bond force per unit length, p_d the perimeter of the reinforcement of size d and λ the reciprocal slope of the linear bond force vs. relative displacement function, normally available with semiempirical values [22], we obtain:

$$B_k = \frac{p_d h}{\Lambda}.$$

In knowledge of the solution, the bond shear stress is delivered by these relationships. In the case of a vertical or horizontal reinforcement ending in the node, the main diagonal block affecting the nodal stiffness characteristics of the concrete unit is:

$$B_{kv} \begin{bmatrix} 1/2 & 0 \\ 0 & 0 \end{bmatrix}, \quad \text{symbol } k'_{kv} \quad \text{and} \quad B_{kf} \begin{bmatrix} 0 & 0 \\ 0 & 1/2 \end{bmatrix}, \quad \text{symbol } k'_{kf}.$$

Blocks of reinforcement crossing the node are $k_{kv} = 2k'_{kv}$ and $k_{kf} = 2k'_{kf}$.

3.23 Effect of the reinforcement tied to the node on the nodal stiffness

In the case of a model of a concrete unit with horizontal or vertical reinforcement ending at the node, the blocks along the main diagonal are $k_i + k'_{0kv}$ and $k_i + k'_{0kv}$ resp., and for reinforcement continuous over the node $k_i + k_{0kf}$ and $k_i + k_{0kf}$ resp., (Figs 9 and 10), where k_i is the block of bars simulating the concrete as described earlier. The main diagonal block at the nodal point where ties and horizontal and vertical reinforcements ending in the node join $k'_{0kv} + k_{0\blacksquare v}$, symbol k'_v; and $k'_{0kf} + k_{0\blacksquare f}$, symbol k'_f and in the case of continuity of the reinforcement $k_{0kv} + 2k_{0\blacksquare v}$, symbol $k_{v\blacksquare}$ and $k_{0kf} + 2k_{0\blacksquare f}$, symbol $k_{f\blacksquare}$. Blocks off the main diagonal are those in items 3.21 and 3.22 accordingly.

3.24 Stiffness matrix of the model of a reinforced concrete member

Simulating the bond by ties, common points of reinforcement and ties are as many new points of the grid. Accordingly, the number of unknowns grows, and so does the size of the stiffness matrix.

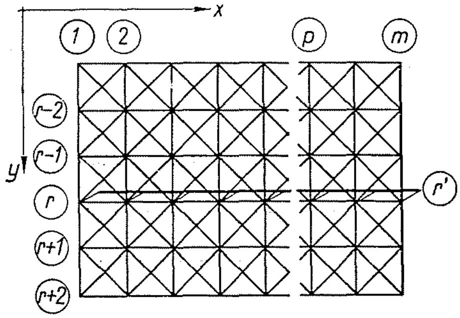

Fig. 9

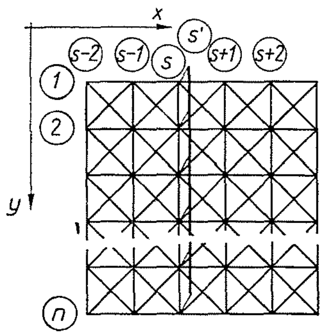

Fig. 10

3.241 The case of a horizontal reinforcement

For a horizontal reinforcement leading between both ends of the member and connected elastically to all points of a row of nodes (e.g. r in Fig. 9) the stiffness matrix in item 3.13 becomes as follows.

To every 2×2 size block with a subscript r, r of main diagonal $2n \times 2n$ blocks is added a block $k_{k\nu}$ at an arbitrary point of the reinforcement, or a block $k'_{k\nu}$ at the steel end (the first and m-th blocks $\mathbf{A}^{I}_{\nu}$ and $\mathbf{A}^{II}_{\nu}$, resp., in Fig. 9). Block column r contains blocks $n \times m$, and an $m \times m$ one in the main diagonal (of course, these are hypermatrices with 2×2 blocks). From the first m blocks of the block column r', elements with subscripts r, p of the p-th block $\mathbf{V}_{\nu p}$ equal v_k, and v'_k, the others are zero. The main diagonal of the $m \times m$ type block $\mathbf{V}_{\nu p}$ includes k_ν (in the corners k'_ν), and codiagonals have v. Thus, the stiffness matrix becomes:

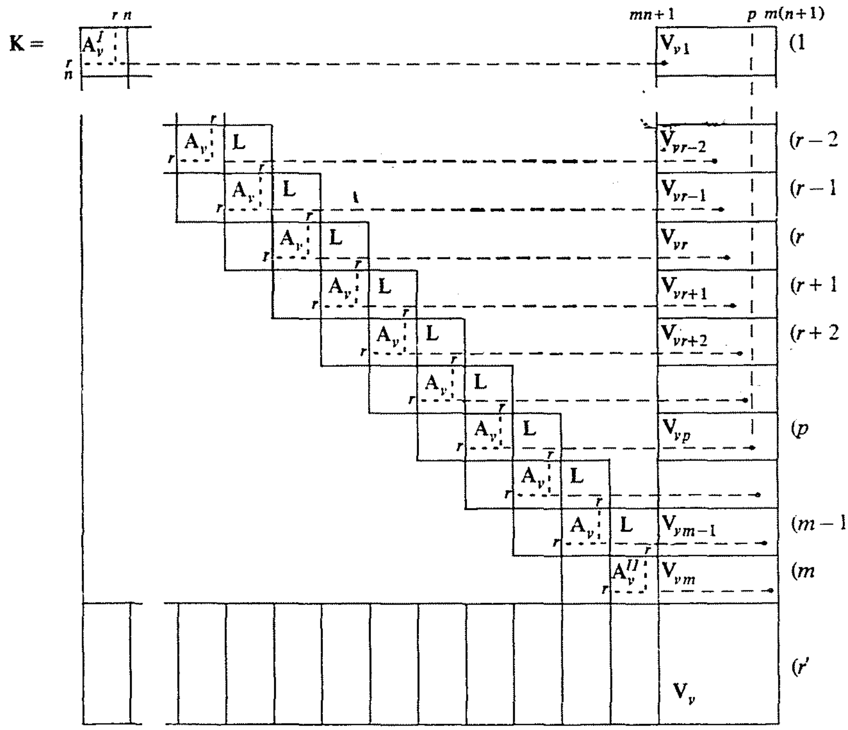

3.242 The case of vertical reinforcement

Stiffness matrix of the model of a vertical reinforcement (stirrup) continuous throughout the structural height at line s (see Fig. 10) differs from that in item 3.13 by the following. Main diagonal block of the s-th block column is

$$\mathbf{V}_{bf} = \mathbf{A} + \langle k'_{kf}, k_{kf}, \ldots, k_{kf}, k'_{kf} \rangle = \mathbf{A} + \mathbf{D}_{kf}.$$

Only the s-th block and that in the main diagonal of the $m + 1$-th block column s' are non-zero.

The s-th block is:

$$\mathbf{V}_{kf} = \langle f'_k, f_k, \ldots, f_k, f'_k \rangle = \mathbf{V}^T_{kf},$$

and the last one in the main diagonal:

$$\mathbf{V}_f = \mathbf{D}_{\blacksquare f} + f_{\blacksquare}\mathbf{C},$$

where:

$$\mathbf{D}_{\blacksquare f} = \langle k'_{f\blacksquare}, k_{f\blacksquare}, \ldots, k_{f\blacksquare}, k'_{f\blacksquare} \rangle,$$

and

$$\mathbf{C}=\begin{bmatrix} 0 & 1 & & & & \\ 1 & 0 & 1 & & & \\ & \ddots & \ddots & \ddots & & \\ & & \ddots & \ddots & \ddots & \\ & & & 1 & 0 & 1 \\ & & & & 1 & 0 \end{bmatrix}.$$

Finally, the stiffness matrix becomes

$$\mathbf{K}=\left[\begin{array}{cccccccccccc}
\mathbf{A}^{I} & \mathbf{L} & & & & & & & & & & \\
\mathbf{L}^{T} & \mathbf{A} & \mathbf{L} & & & & & & & & & \\
 & \ddots & \ddots & \ddots & & & & & & & & \\
 & & \mathbf{L}^{T} & \mathbf{A} & \mathbf{L} & & & & & & & \\
 & & & \mathbf{L}^{T} & \mathbf{A} & \mathbf{L} & & & & & & \\
 & & & & \mathbf{L}^{T} & \mathbf{V}_{bf} & \mathbf{L} & & & & & \mathbf{V}_{kf} \\
 & & & & & \mathbf{L}^{T} & \mathbf{A} & \mathbf{L} & & & & \\
 & & & & & & \mathbf{L}^{T} & \mathbf{A} & \mathbf{L} & & & \\
 & & & & & & & \ddots & \ddots & \ddots & & \\
 & & & & & & & & \mathbf{L}^{T} & \mathbf{A} & \mathbf{L} & \\
 & & & & & & & & & \mathbf{L}^{T} & \mathbf{A}^{II} & \\
 & & & & & \mathbf{V}_{kf}^{T} & & & & & & \mathbf{V}_{f}
\end{array}\right]
\begin{array}{l}
(1 \\ \\ \\ (s-2 \\ (s-1 \\ (s \\ (s+1 \\ (s+2 \\ \\ (m-1 \\ (m \\ (s'
\end{array}$$

3.25 Model stiffness for cracked reinforced members

In simulating cracking by cutting bars of the model of the concrete, statements in items 3.14 and 3.23 are valid, namely k_i may stand for any possible nodal stiffness of the concrete model.

3.26 Bond of a non-linear relationship

We do not intend to deal with the problem to the extent how the computation is suitable to take the plasticity characteristics of the concrete into consideration by means of considering the yield of given bars of a framework simulating the continuum.

Only the formation of nodal displacements and internal forces in the case of the yield of several bars, e.g. of ties, hence a constant bond force T_F for varying displacement will be examined, instead of the linear relationship between bonding force and relative displacement. The presented relationships can be generalized for multi-parameter loads, nevertheless $\mathbf{q}$ will be considered below to have a single parameter q. Let q_0 be the yield parameter of the first bar with end points j, k, then nodal displacements can be written as

$$\mathbf{K}\mathbf{u}_0 = q_0\mathbf{q}\,.$$

Bar i, j is inoperative for a load higher than q_0 determined from the solution $\mathbf{u}_0$ ($\Delta u_{ij} = \Delta u_{ijF}$) but develops a constant force T_F. $\mathbf{K}''$ is a modified stiffness matrix ignoring the stiffness of bar j, k. Displacement vector $\mathbf{u}$ for $q > q_0$ is delivered by

$$\mathbf{K}''\mathbf{u}'' = \mathbf{K}''(\mathbf{u} - \mathbf{u}_0) = (q - q_0)\mathbf{q}.$$

Displacements are the sum

$$\mathbf{u} = \mathbf{u}_0 + \mathbf{u}''.$$

This equation is equivalent to

$$\mathbf{K}''\mathbf{u} = q\mathbf{q} + \mathbf{q}_m,$$

where $\mathbf{q}_m$ is a vector with non-zero elements of value T_F occurring at the point of the yield (or the phenomenon simulated by it), at nodes of yielded bar ends ([24]).

4. The elastic spatial model

Here we intend only to show that the spatial model built up from elements seen in Fig. 12 can be treated similarly to the plane problem.

Merely a spatial grid is seen in Fig. 11. As an illustration, stiffness matrix of the model of the prism spanning between lines n, m, p in directions x, y, z is

$$\mathbf{K} = \begin{bmatrix} \mathbf{A}^I & \mathbf{L} & & & & \\ \mathbf{L}^T & \mathbf{A} & \mathbf{L} & & & \\ & & \ddots & & & \\ & & & \ddots & & \\ & & & \mathbf{L}^T & \mathbf{A} & \mathbf{L} \\ & & & & \mathbf{L}^T & \mathbf{A}^{II} \end{bmatrix}$$

As an example, hypermatrix block $\mathbf{A}$ of size $m \times m$, one of those contained in the matrix is

$$\mathbf{A} = \begin{bmatrix} \mathbf{B}^I & \mathbf{L} & & & & \\ \mathbf{L}^T & \mathbf{B} & \mathbf{L} & & & \\ & & \ddots & & & \\ & & & \ddots & & \\ & & & \mathbf{L}^T & \mathbf{B} & \mathbf{L} \\ & & & & \mathbf{L}^T & \mathbf{B}^{II} \end{bmatrix}$$

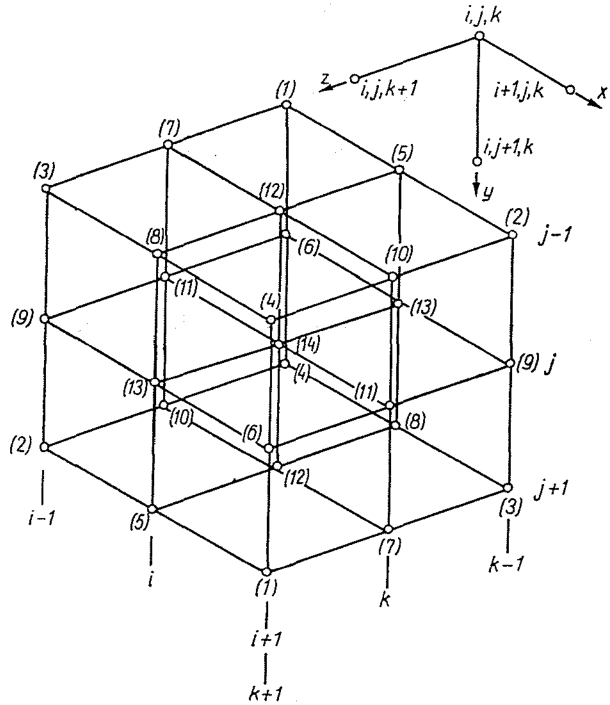

Fig. 11

yielding matrix **B**, again as an example:

$$
\mathbf{B} = \begin{array}{cl}
\left[\begin{array}{cccccccccccc}
k_{12} & f & & & & & & & & & & \\
f & k_{14} & f & & & & & & & & & \\
 & f & k_{14} & f & & & & & & & & \\
 & & \cdot & \cdot & \cdot & & & & & & & \\
 & & & \cdot & \cdot & \cdot & & & & & & \\
 & & & & \cdot & \cdot & \cdot & & & & & \\
 & & & & & f & k_{14} & f & & & & \\
 & & & & & & f & k_{14} & f & & & \\
 & & & & & & & f & k_{14} & f & & \\
 & & & & & & & & \cdot & \cdot & \cdot & \\
 & & & & & & & & & \cdot & \cdot & \cdot \\
 & & & & & & & & & & f & k_{12}
\end{array}\right] &
\begin{array}{l}
((m+1)n+1 \\ \\ \\ \\ \\ \\ \\ \\ \\ \\ \\ ((m+2)n
\end{array}
\end{array}
$$

Matrix elements are blocks type 3×3 that may be compiled by analogy to the plane case. Blocks in the main diagonal contain the local stiffness matrices of the zones or the biplanar bars written in the global co-ordinate system.

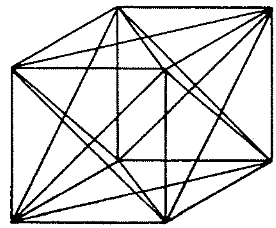

Fig. 12

Obviously, secondary diagonal blocks contain a single non-zero element, hence in the example of a block **B**:

$$f = \frac{EA_y}{h} \begin{bmatrix} 0 & 0 & 0 \\ 0 & -1 & 0 \\ 0 & 0 & 0 \end{bmatrix}.$$

5. Support, loads and prestressing forces

All row sums of the stiffness matrix **K** for different cases are zero, hence the matrix is a singular one. Supporting a model node, i.e. preventing its displacement in directions x, y and z, the corresponding row or column of the matrix has to be cancelled. In the case of supports in a due number and position (e.g. at least three of different directions in the plane) the stiffness matrix will not be a singular one. Of course, loads may only act at nodes. Simulating the nodes, reckoning with the reality of not truly concentrated loads has to be attempted by way of some approximation, and so it has in the case of the reactions.

Prestress acting on post-tensioned beams may be considered as an external force, omitting prestress decrease due to elastic deformation.

As a matter of fact, the prestressing effect in pre-tensioned beams can be taken into consideration by making use of the displacement method — similarly to the real processes on the prestressing bed. For a prestressing tendon of direction x crossing a node, the statement on the node equilibrium (an equation in the set) will be written by replacing displacement u_x by $u_x + e_f$, where e_f is the tendon elongation per mesh due to prestress.

6. Stress determination from model node displacements

In knowledge of the displacement vector, bar elongations, and hence, in knowledge of stiffness, the bar forces can be determined.

Stress analysis may follow grouping in Fig. 13 (tie effect resulting from the nodal equilibrium).

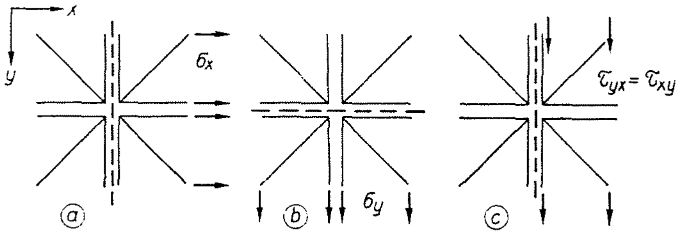

Fig. 13

7. Example of applying the mathematical model

Determination of the forces and reactions in a stepped post-tensioned beam end will be presented as an example. The cantilever of this beam has previously been analyzed by a different method, and the entire beam end has been tested up to failure ([26]).

7.1 *Beam end data*

Lateral view of the beam end with the grid is seen in Fig. 14 ($h = 5$ cm), the member considered as a plane problem has a thickness of 40 cm. $E_b = 4.6 \times 10^5$ kp/cm². Reinforcement cross sections and perimeters have been

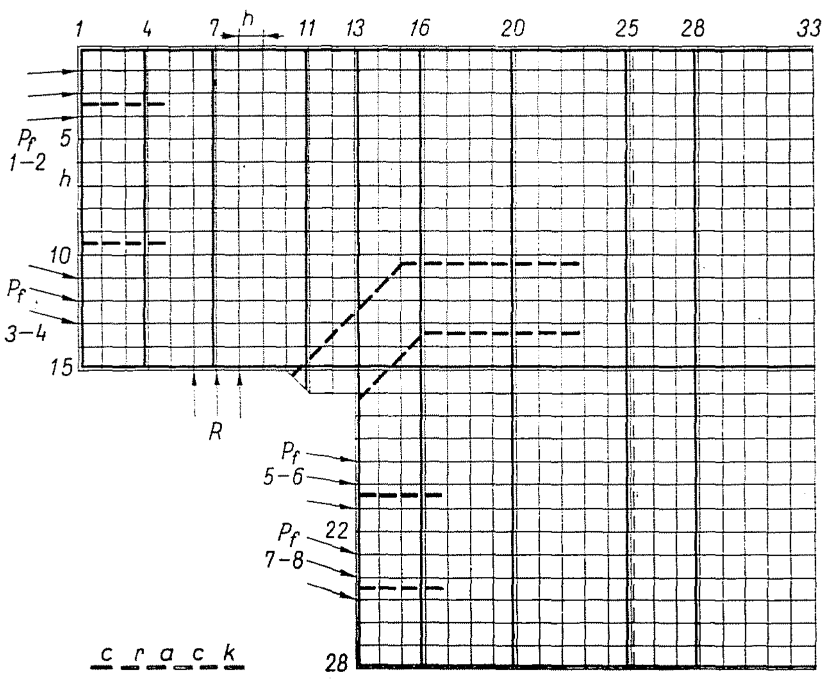

Fig. 14

Table IV

Symbol		P_{f1-2}			P_{f3-4}			P_{f4-5}			P_{f7-8}			R	
	a	b	c	a	b	c	a	b	c	a	b	c	a	b	c
The force application point i	1	1	1	1	1	1	13	13	13	13	13	13	6	7	8
j	2	3	4	11	12	13	19	20	21	23	24	25	15	15	15
Components (Mp) x	36.43	36.43	36.43	35.23	35.23	35.23	36.02	26.02	36.02	36.42	36.42	36.42	0	0	0
y	−1.59	−1.59	−1.59	9.44	9.44	9.44	5.70	5.70	5.70	1.91	1.91	1.91	−5.97	−5.97	−5.97

converted according to the model law of similitude. Longitudinal reinforcements and stirrups are equal in diameter and in number for one section:

$$A_{\blacksquare v} = A_{\blacksquare f} \approx 7 \text{ cm}^2; \quad p_d \approx 19 \text{ cm}; \quad E_a = 2.1 \times 10^6 \text{ kp/cm}^2.$$

Prestress and reaction due to external loads have been replaced by three parallel components. Forces between the beam end and the adjacent beam part have been accounted for according to the mathematical model. To validify the de Saint-Venant principle, beyond the 25th column in Fig. 14 — at the beam end butt — further 8 divisions have been assumed. Load arrangement is seen in Fig. 14, and load values have been compiled in Table IV.

7.2 *The mathematical model*

The beam end in item 7.1 has a boom stiffness $B = 13.77 \times 10^6$ kp/cm² in directions both x and y, with a diagonal stiffness coefficient $\beta = 0.5$. Reinforcement stiffness is $B_{\blacksquare} = 2.92 \times 10^6$ kp/cm². The bond coefficient has been assumed as $\Lambda = 1/400$ cm³/kp. Accordingly $B_k = 37.7 \times 10^3$ kp/cm².

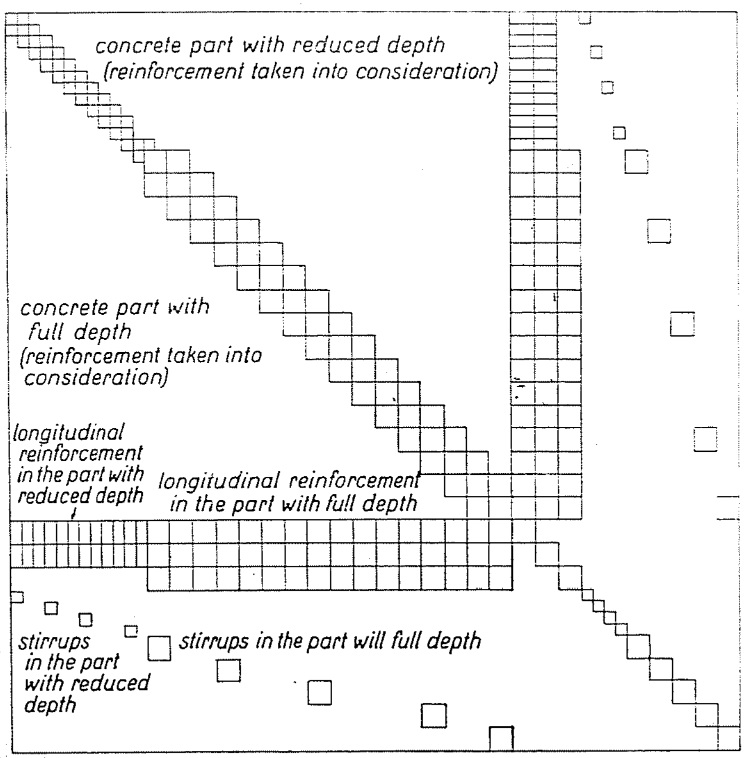

Fig. 15

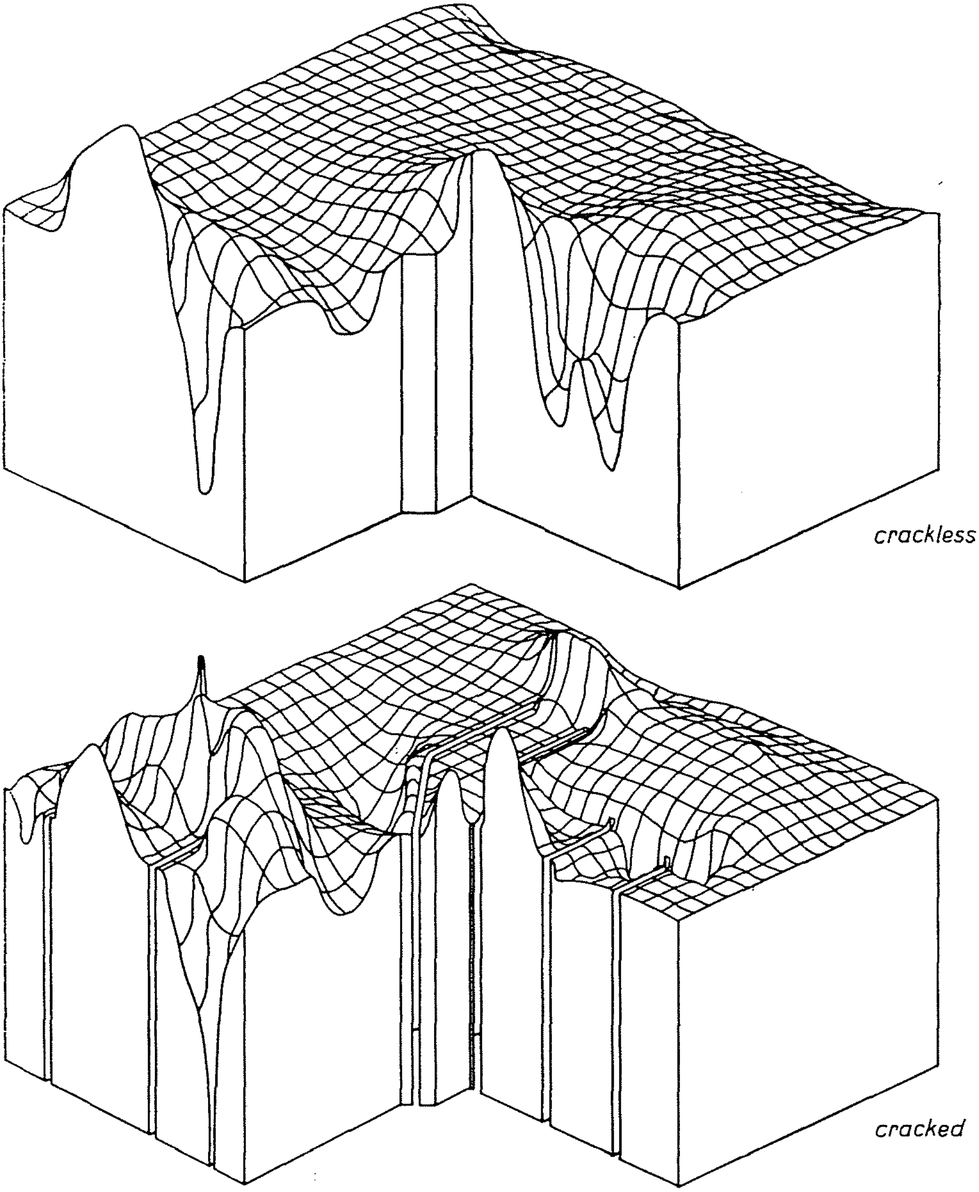

Fig. 16

In the first group of solutions, the concrete has been considered as exempt of cracks but reinforced. Cracks have been taken into account according to item 3.14, by approximation based on test results ([25]), and represented in dash line in Fig. 14. There are 1058 nodes in the model, of them 770 simulate the concrete member, 87 the end points of the longitudinal ties, and 201 those of the stirrup ties.

Details of the computer analysis will be omitted here. Scheme of the coefficient matrix of the set of equations solving the model in Fig. 14 by the displacement method is seen in Fig. 15. (Non-zero blocks have been framed.)

7.3 *Computation results*

Computation resulted in model nodal stresses σ_x, σ_y and τ_{xy}, longitudinal steel and stirrup stresses, bond stresses in all crack-free and cracked units, and crack width.

As an example, development of stresses σ_y, will be presented both for the crack-free and the cracked beam. In Fig. 16 stress redistribution due to cracking is seen in the axonometric picture of the member with cracks traced in dashed lines in Fig. 14.

8. Conclusions

Advantages of the framework analogy model of reinforced or prestressed concrete members appear even in case of certain limitations. The model suits to simulate the cracking, the reinforcement, the bond. Applicability of the model is demonstrated by means of an example.

Summary

A mathematical model has been constructed, suitable to simulate a concrete member in stress states I and II, to consider reinforcement and cracking, and also effects of certain plastic behaviour. Stiffness matrices of the concrete unit, the cracked concrete unit and the reinforced concrete unit are written for the model based on the extended framework analogy, involving the methods of the bar system theory. Concrete to steel bond simulation, establishment of spatial models, simulation of supports, external forces and prestress have been considered. The method has been illustrated on the example of a stepped, post-tensioned beam end with longitudinal steel and stirrups, in crack-free and cracked conditions.

References

1. Mihailich, Gy.—Schwertner, A.—Gyengő, T.: Theory and Design of Reinforced Concrete Structures.* Németh J. Könyvk., Budapest, 1946.
2. Mihailich, Gy.—Palotás, L.: Reinforced Concrete Construction. I. Theory of Reinforced Concrete.* Tankönyvkiadó, Budapest, 1964.
3. Almási, J.: Wieviel Spaltzugbewehrung ist nötig? IVBH Abhandlungen 35-II. (1975) pp. 15—27
4. Ban, S.: Anchorage Zone Stress Distributions in Post-Tensioned Concrete Members. Proceedings of the World Conference on Prestressed Concrete, San Francisco, 1957.
5. Bölcskei, E.—Orosz, Á.: Reinforced Concrete Structures. Deep Beams, Plates, Reservoirs.* Tankönyvkiadó, Budapest, 1972.
6. Bölcskei, E.—Szalai, K.: Reinforced Concrete Structures. Theory of Reinforced Concrete.* Tankönyvkiadó, Budapest, 1974.
7. Christodoulides, S. P.: A Three-Dimensional Investigation of the End Anchorages of Post-Tensioned Concrete Beams. Struct. Eng., 33 (1955) pp. 120—133

* In Hungarian

8. CHRISTODOULIDES, S. P.: Three-Dimensional Investigation of the Stresses in the End Anchorage Blocks of a Prestressed Concrete Gantry Beam. Struct. Eng., 35 (1957) pp. 339—356
9. GUYON, Y.: Béton précontraint. Eyrolles, Paris, 1951.
10. HEGEDŰS, I.: Analysis of Substituting Continuum of Spatial Lattice Works.* Doctor Techn. Thesis, BME Budapest, 1972.
11. HIGASHIDA, K.—NAKAJIMA, N.: Experimental Study on Reinforcement of Multiple Anchorage Zone in Post-Tensioned Concrete Members. J. Japan Prestr. Concr. Eng. Ass. 16 (1974) 5. pp. 41—47
12. HRENNIKOFF, A.: Solution of Problems of Elasticity by the Framework Method. J. Appl. Mech. 1941. pp. 169—175
13. HRENNIKOFF, A.—GANTAYAT, A.: The Three-Dimensional Bar Cell of Elastic Stress Analysis. J. ASCE, EM3 (1970) pp. 313—326
14. KOLLÁR, L.—HEGEDŰS, I.: A Continuous Mathematical Model for Two-Layer Structures with General Triangle Grid.* Műszaki Tudomány 46 (1973) pp. 53—70
15. McCORMICK, C. W.: Plain Stress Analysis. J. ASCE, ST4 (1963) 37—52 pp.
16. НОСАРЕВ, А. В.: О напряжениях в хомутах железобетонных предварительно напряженных пролетных строений с наклонной трещиной в стенке. МИИТ 344 (1971) pp. 51-62.
17. SARGIOUS, M.—TADROS, G. S.: Stresses in Pre-Tensioned Concrete Stepped Cantilevers under Concentrated Loads. FIP 6th Congress, Praha 1970.
18. SCHWARZ, H.—HAAS, F. O.: Anwendung der Stabwerkmethode zur Lösung des ebenen Spannungsproblems. Die Bautechnik, 1968. pp. 200—205
19. SCHWERTNER, A.: Versuche zur Bestimmung der Kräfte, welche an der Mantelfläche von einbetonierten Eisen- oder Stahleinlagen übertragen werden. Acta Technica Acad. Sci. Hung. Tom. II. (1951).
20. TASSI, G.: The Theory of Self-Anchorage of Prestressed Tendons in Concrete.* Építés- és Közl. Tud. Közl. 1959. 1—2. pp. 217—258
21. TASSI, G.: Analysis of a One-Dimensional Mathematical Model of a Bar of two Connected Elements.* BME Ép. m. Kar, Építőanyagok Tsz. Tud. Közl. 21 (1975) 141—166 p.
22. TASSI, G.: Experimental Research on the Self-Anchorage of Prestressing Steel.* Építés- és Közl. Tud. Közl. 1960. 1—2. pp. 235—265
23. TASSI, G.: The Possibility of Anchorage on Finite Length in Pre-Tensioned Prestressed Concrete. Sc. Publ. of the Techn. Univ. of Bdg. and Transp. Eng. Extr. Sci. Wks, Dept. of Bridge Constr. II (1957) pp. 41—50
24. TASSI, G.: Contribution to the Analysis of Stiffness and Cracking Conditions of Prestressed Concrete Members. FIP VIIIth Congress, London 1978.
25. TASSI, G.—WINDISCH, A.: Model Tests on Post-Tensioned End-Block Elements.* Congr. Prefabr. in Civil Eng. Final Vol. KÖZDOK, Budapest, 1973. pp. 23—25
26. TASSI, G.—WINDISCH, A.: Analysis and Model Testing of the Anchorage Zone of Post-Tensioned Beams. FIP VIIth Congress, New York 1974.
27. WINDISCH, A.—KISBÁN S.: A Two-Dimensional Investigation of the Distribution of Stresses in the End Blocks of Prestressed Concrete Beams. ÉTI Bulletin 12 (1974) pp. 26—49
28. YETTRAM, A. L.—ROBBINS, K.: Anchorage Zone Stresses in Axially Post-Tensioned Members of Uniform Rectangular Section. Mag. Concr. Res. 21 (1969) pp. 103—112
29. YETTRAM, A. L.—ROBBINS, K.: Anchorage Zone Stresses in Post-Tensioned Uniform Members with Eccentric and Multiple Anchorages. Mag. Concr. Res. 22 (1970) pp. 209—218
30. ZIELINSKI, J. L.—ROWE, R. E.: An Investigation of the Stress Distribution in the Anchorage Zones of Post-Tensioned Concrete Members. Cement and Concr. Ass. London, 1960.

Professor Géza TASSI, D. Techn. Sc. H—1521 Budapest

* In Hungarian.